

# Characterization of the rheological behavior wood cell-wall through nanoindentation

Moisés Gresve<sup>1</sup>, Juan Carlos Pina<sup>1</sup>, Carlos Felipe Guzmán<sup>1</sup>

<sup>1</sup>Civil Engineering Department, Faculty of Engineering, University of Santiago (USACH), Chile.

## Resumen

Este estudio se centra en investigar las propiedades mecánicas de la pared celular de la madera, específicamente la capa S2, utilizando el método de elementos finitos con un modelo constitutivo higo-viscoelástico desarrollado en el software FEniCS. La metodología consiste en simular el ensayo de nanoindentación mediante el software ANSYS Structures y calibrar el modelo con resultados experimentales disponibles en la literatura. Posteriormente, se realiza una comparación del creep y la relajación utilizando tanto ANSYS como FEniCS, con el objetivo de que el modelo permita predecir un conjunto de parámetros que describen la capa S2 en función de la humedad.

**Palabras clave:** Madera, Higo-viscoelasticidad, Capa S2, Nanoindentación

## Abstract

This study focuses on investigating the mechanical properties of the wood cell wall, specifically the S2 layer, using the finite element method with a hygro-viscoelastic constitutive model developed in FEniCS software. The methodology involves simulating the nanoindentation test using ANSYS Structures and calibrating the model with experimental results available in the literature. Subsequently, a comparison of creep and relaxation is carried out using both ANSYS and FEniCS, with the aim of enabling the model to predict a set of parameters describing the S2 layer as a function of moisture.

**Keywords:** Wood, Hygro-viscoelastic, S2 Layer, Nanoindentation

## 1. Introduction

Despite the significant advancements that wood has experienced in the field of construction, it is essential to continue studying this material for its application in large-scale constructions. One factor that can considerably influence the mechanical properties of wood, such as its stiffness, strength, and ductility, is the presence of moisture. In structural design, the impacts of moisture are accounted for through an adjustment factor that alters the mechanical properties of the wood, according to Chilean standard [1], in addition to considering other safety factors that reduce the initial strength.

On the other hand, creep and relaxation phenomena are increased by moisture. Creep, where deformation increases with the duration of the applied load, is intensified in the presence of moisture. Similarly, when wood is subjected to a constant deformation, the initial

stress gradually decreases over time. This behavior is known as relaxation.

Wood is structured hierarchically at macro, micro, and nano scales. At the cellular level, water is present in three distinct phases within its structure. These phases include water bound in the cell wall, water vapor, and free water (known as capillary water) in the lumen [2].

Therefore, it is interesting to study the different components present in the cell wall and how these mechanical properties are affected by varying moisture content (MC). The cell wall, and specifically the S2 layer, is composed of a fibrous matrix. In this matrix, lignin and hemicelluloses form the matrix, while the fibers consist of crystalline and amorphous cellulose.

Cousins [3] demonstrated that both the Young's modulus and the shear modulus decrease linearly as the moisture content (MC) increases. Additionally,

Cousins [4] showed that hemicellulose is more sensitive to changes in moisture content compared to cellulose and lignin. This is also mentioned in the article by L. Salmén [5].

There are few articles that address the study of these wood properties through numerical modeling. Among them, Meng [6] and Hayot [7] stand out for their experimental and numerical analysis of the viscoelastic properties of the S2 layer.

In this work, a hygroviscoelastic model is proposed for the S2 layer of the cell wall, with parameters obtained through nanoindentation simulations. For this, indentation simulations are performed under different moisture contents, and the viscoelastic parameters are obtained using a Maxwell model, similar to the approach used in Meng's study. These parameters are then used to derive creep and relaxation curves, which are analyzed using the proposed model.

## 2. Rheological model of the S2 layer.

Currently, there is work done by (Lazo-Molina and Guzman) [8], where a multiphysical numerical model is developed specifically for this layer, as a nanocomposite consisting of a matrix and fibers. The matrix, composed of hemicellulose, lignin, and water, is reinforced with cellulose fibrils. The model addresses mechanosorption, water diffusion in the polymer network, and viscoelasticity due to mechanical stresses. It also considers the mechanical contribution of cellulose fibrils, describing the elastic behavior of crystalline cellulose and its viscoelastic behavior in the amorphous form. The model is implemented using the open-source finite element software with symbolic capabilities FEniCS [9]. A detailed description of the model's formulation, implementation, and validation will be the subject of a future publication.

The energy functional is defined as follows:

$$\Psi = (1 - v_f) \cdot [\Psi_e^m + \Psi_{mix} + \Psi_v^m] + v_c \cdot \Psi_e^f + v_a \cdot \Psi_v^f \quad (1)$$

Donde:

- $\Psi_e^m$  : elastic of the matrix
- $\Psi_{mix}$  : interaction between matrix polymers
- $\Psi_v^m$  : viscoelastic of the matrix
- $\Psi_e^f$  : elastic of the fiber
- $\Psi_v^f$  : viscoelastic of the fiber
- $v_c, v_a$  : Volume fraction of crystallized and amorphous cellulose

The mechanical properties of the model under study are detailed in **Table 1**, where the analyzed properties are highlighted in blue.

To study the different components of the S2 layer, the methodology outlined in **Fig. 1** will be employed. Initially, the wood of the Loblolly pine species (*Pinus taeda* L.) will be analyzed using both experimental results and simulations described in the article by Meng [6].

Once the parameters are validated in ANSYS, a three-dimensional model of a cube with the same dimensions will be developed in both ANSYS and FEniCS. This is done to avoid the specific contact issues of the FEniCS software. After correlating both models, creep and relaxation tests will be conducted for analysis.

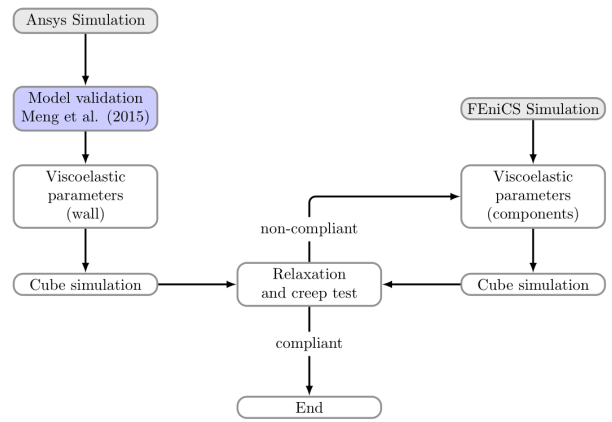


**Fig. 1.** Methodology: The approach includes two branches: simulation using ANSYS and simulation using FEniCS, corresponding to the parameters of the S2 layer and the mechanical properties of its components.

The objective is to define a set of parameters for layer S2, such that the model can predict the variation in Young's modulus with respect to moisture.

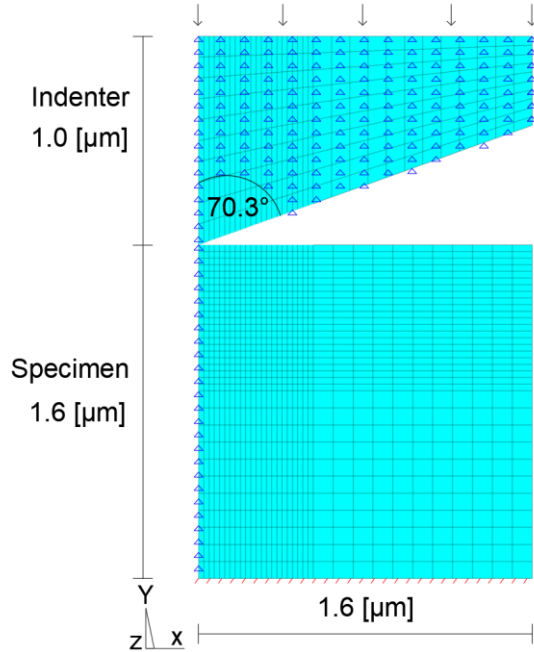
### 2.1. Model validation

Similarly to the simulation described by Meng [6], an axisymmetric model along the y-axis is created using PLANE183 elements and employing ANSYS APDL, as shown in **Fig. 2**. The simulation involves applying a 250  $\mu\text{N}$  load for 5 seconds, followed by maintaining it constant for another 5 seconds. The boundary conditions are as follows: the bottom ( $y=0$ ) is fixed, nodes on the axis ( $x=0$ ) are constrained to  $x=0$ , and all nodes on the loading element are also constrained in  $x=0$ . A distributed load of 250  $\mu\text{N}$  is applied to the surface of the element. The Young's modulus and Poisson's ratio for this element are 1140 GPa and 0.07, respectively. As in the article, two Prony series are used with the Maxwell model, where the relative

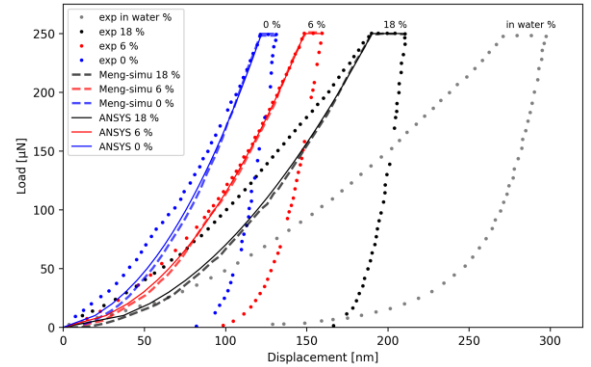
**Table 1.** Input parameters of the constitutive model.

| Table Model Input Parameters |                            |              |                                   |
|------------------------------|----------------------------|--------------|-----------------------------------|
| Constituent                  | Parameter                  | Nomenclature | Unit                              |
| Cellulose fibril             | Orientation of the fibrils | MFA          | degrees                           |
|                              | Total volume fraction      | $v_f$        | %                                 |
| Crystalline cellulose        | Volume fraction            | $v_f$        | kPa                               |
|                              | Shear modulus              | $G_e^f$      | %                                 |
|                              | Poisson's ratio            | $\nu$        | -                                 |
| Amorphous cellulose          | Volume fraction            | $v_f$        | %                                 |
|                              | Shear modulus              | $G_e^f$      | kPa                               |
| Matrix                       | Shear modulus              | $G_e^f$      | kPa                               |
|                              | Shear modulus              | $G_e^f$      | kPa                               |
|                              | Bulk modulus               | $k$          | kPa                               |
|                              | Poisson's ratio            | $\nu$        | -                                 |
|                              | Viscosity                  | $\eta$       | kPa·s                             |
| Diffusion                    | Volume per mole of water   | $\Omega$     | mm <sup>3</sup> mol <sup>-1</sup> |
|                              | Permeability               | $\kappa$     | mm <sup>2</sup>                   |
|                              | Water viscosity            | $\eta_w$     | kPa·s                             |
|                              | Interaction parameter      | $\chi$       | -                                 |

moduli are  $\alpha_1=\alpha_2=0.5$ . The relaxation times  $\tau_1$  and  $\tau_2$ , along with the different Young's modulus values calculated in the article, are provided in **Table 2**. The column highlighted in blue corresponds to the results obtained in the current simulation. A linear material is used for the indenter, and a Neo-Hookean visco-hyperelastic material is used for the sample.

**Fig. 2.** Axisymmetric Finite Element Modeling: Mesh Configuration, Dimensions, Boundary Conditions, and Loading Conditions.

**Fig. 3** shows the experimental and numerical results from the mentioned study, along with the fit from the current simulation. A good correlation between the experimental data and the simulation results is observed. On the other hand, **Fig. 4** displays the creep compliance curves along with the simulation results. A good correlation is observed for the curves with 0% and 6% moisture content, but this is lost for the 18% moisture curve, indicating the need to adjust the simulation parameters to improve agreement with the experimental data.

**Fig. 3.** Nanoindentation.

The creep compliance curve is obtained by applying a load of 250  $\mu\text{N}$  for 5 seconds using the indenter. The displacements recorded during the simulation are used in Equation (2), where  $P_0$  is the initial load. The parameter  $\nu$  is the Poisson's ratio and  $\delta$  is the indenter's opening angle ( $70^\circ$  for the Berkovich indenter).

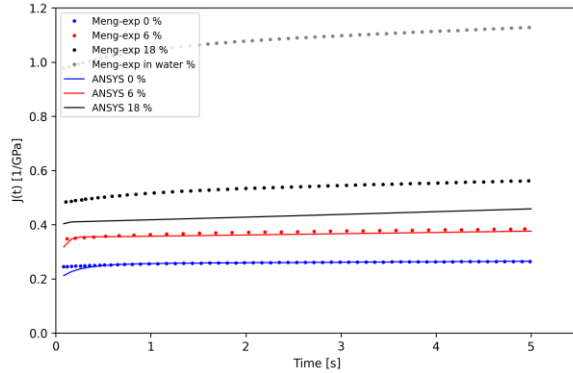
**Table 2.** Elastic Moduli and Relaxation Times for Different Moisture Contents.

| Table Elasticity and Relaxation Data |                            |                         |  |              |              |                        |
|--------------------------------------|----------------------------|-------------------------|--|--------------|--------------|------------------------|
| Moisture content (%)                 | E from Burgers model (GPa) | E from O-P method (GPa) | E from the Generalized Maxwell model (GPa) | $\tau_1$ (s) | $\tau_2$ (s) | Simulation Ansys (GPa) |
| 0                                    | 10.5                       | 13.9                    | 14.4                                       | 0.13         | 45           | 12.9                   |
| 6                                    | 8.3                        | 12.4                    | 11.5                                       | 0.05         | 30           | 8.8                    |
| 18                                   | 6.3                        | 9.4                     | 9  | 0.01         | 16           | 5.5                    |
| water                                | 2.9                        | 4.5                     | N/A  | N/A          | N/A          | N/A                    |

Source: Elastic moduli reported by Meng [6].

The contact area  $A(t)$  is related to the depth of penetration of the indenter through a function described by a polynomial in the article.

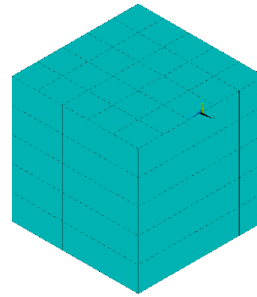
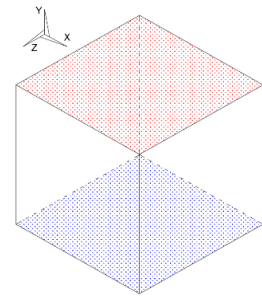
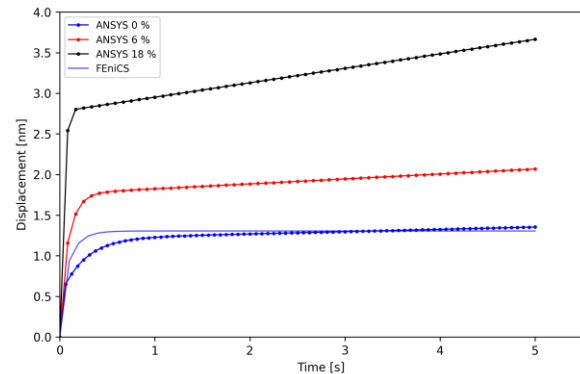
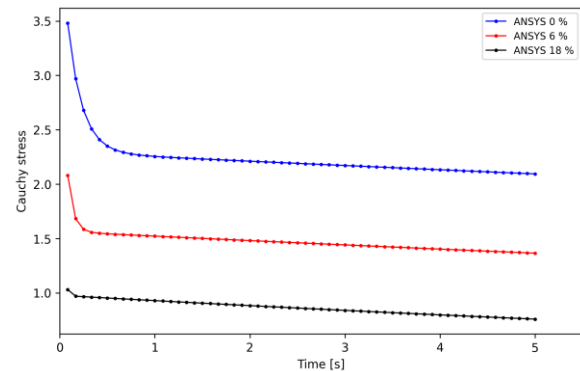
$$J(t) = \frac{1}{2 \cdot (1-\nu^2) \cdot \tan(\delta)} \frac{A(t)}{P_0} \quad (2)$$

**Fig. 4.** Creep compliance.

## 2.2. Creep and relaxation test

First, a simulation of a cube with dimensions of  $1.25 \mu\text{m}^3$  is conducted in ANSYS in ANSYS using the SOLID185 element (see **Fig. 5**), using the properties obtained from the creep and relaxation tests, and in FEniCS with properties derived from the literature. The boundary conditions are illustrated **Fig. 6**. In this figure, the blue segment is fixed, while the red segment has applied load or displacement conditions to assess the creep or relaxation behavior, respectively. For the creep test, a compression load of  $250 \mu\text{N}$  is applied, whereas for the relaxation test, a displacement of  $0.4 \mu\text{m}$  in the positive direction is applied.

**Fig. 7** and **Fig. 8** present the results of creep and relaxation for various moisture contents. In **Fig. 7**, a preliminary curve for the proposed model is shown, which is still under analysis.

**Fig. 5.** Finite Element Model**Fig. 6.** Boundary Conditions**Fig. 7.** Creep.**Fig. 8.** Relaxation.

## 2.3. Conclusions

The current differences in the elasticity moduli compared to the article can be attributed to several unspecified factors, such as the geometry size. Additionally, the type of fitting procedure used to obtain the relaxation time and Young's modulus parameters is not detailed. These discrepancies may also be due to variations in the types of elements and differences between the software used. Moreover, parameter calibration remains under investigation, given the variability in the adjustable parameter data.

## 3. References

- [1] Instituto Nacional de Normalización, 'Madera — Construcciones en madera — Cálculo (NCh1198.Of2014)', Santiago, Chile: INN, 2014.
- [2] M. Autengruber, M. Lukacevic, and J. Füssl, 'Finite-Element-Based Moisture Transport Model for Wood Including Free Water above the Fiber Saturation Point', *Int. J. Heat Mass Transf.*, vol. 161, p. 120228, Nov. 2020, doi: 10.1016/j.ijheatmasstransfer.2020.120228.
- [3] W. J. Cousins, 'Elastic modulus of lignin as related to moisture content', *Wood Sci. Technol.*, vol. 10, no. 1, pp. 9–17, Mar. 1976, doi: 10.1007/BF00376380.
- [4] W. J. Cousins, 'Young's modulus of hemicellulose as related to moisture content', *Wood Sci. Technol.*, vol. 12, no. 3, pp. 161–167, Sep. 1978, doi: 10.1007/BF00372862.
- [5] L. Salmén, 'Micromechanical understanding of the cell-wall structure', *C. R. Biol.*, vol. 327, no. 9, pp. 873–880, Sep. 2004, doi: 10.1016/j.crv.2004.03.010.
- [6] Y. Meng, Y. Xia, T. M. Young, Z. Cai, and S. Wang, 'Viscoelasticity of wood cell walls with different moisture content as measured by nanoindentation', *RSC Adv.*, vol. 5, no. 59, pp. 47538–47547, 2015, doi: 10.1039/C5RA05822H.
- [7] C. Hayot, E. Forouzesh, A. Goel, Z. Avramova, and J. Turner, 'Viscoelastic Properties of Cell Walls of Single Living Plant Cells Determined by Dynamic Nanoindentation', *J. Exp. Bot.*, vol. 63, pp. 2525–40, Jan. 2012, doi: 10.1093/jxb/err428.
- [8] R. Lazo-Molina and C. F. Guzmán, 'Finite strain rheological model for the wood cell wall. Part I: Constitutive and numerical formulation', in preparation.
- [9] The FEniCS Project, 'FEniCSx Computing Platform', FEniCS Project. Accessed: Dec. 06, 2023. [Online]. Available: <https://fenicsproject.org/>